Response to reviewer #1

Shi and Zhang et al.'s manuscript presents hygroscopicity and mixing state of submicron aerosols at several mobility diameters at Mt. Hua during fall 2021 using HTDMA system. This study presents a valuable and comprehensive dataset on aerosol hygroscopicity in the lower free troposphere over China, supported by concurrent aerosol chemical composition measurements. The manuscript primarily serves as a measurement report based on a robust dataset, rather than providing extensive interpretation or discussion. Given the scientific merit and relevance of the dataset, I believe this manuscript can be considered for publication in Atmospheric Chemistry and Physics after the authors adequately address the following comments and revise accordingly. Most of all, authors are encouraged to related aerosol hygroscopicity, chemical composition, and airmass origins or meteorology impacting aerosol process in the atmosphere.

We greatly appreciate referee#1's positive feedback and constructive suggestions which are of great value for improving the quality of our paper. Below are our point-to-point responses to the referee's comments.

1. L114: The parameter "A" is defined with an equation; however, a clearer explanation of its physical meaning and implications is necessary.

Response:

Thank you for your comment. We realize that the explanation provided in the original manuscript may not have been clear. We have revised the entire formula based on κ-Köhler theory. The revised formula is as follows:

$$\kappa = (GF^3 - 1)\left(1 - \frac{RH}{K_e}K_e\right),$$

$$K_e = \exp\left(\frac{4\sigma_{s/a}M_w}{RT\rho_w D_{dry}}\right),$$

GF is the hygroscopic growth factor measured by HTDMA at 90 % RH. D_{dry} is defined as the particle diameter selected by the first DMA under dry conditions (RH < 10 %) at 25 °C. ρ_w and Mw are the density and molecular weight of water. $\sigma_{s/a}$ is the surface tension of the droplets, which is assumed to be that of pure water ($\sigma_{s/a}$ = 0.0728N m^{-2}). R is the ideal gas constant and T is the ambient temperature, K_e is the Kelvin correction factor term.

2. L115: "Dry" diameter appears to refer to a particle size at 20°C, as suggested in Section 3. Please clarify this here and provide a more detailed explanation.

Response:

Thanks for your specific comment. We have revised the sentence in Line 125 for clarity. The updated sentence now reads: "D_{dry} is defined as the particle diameter selected by the first DMA under dry conditions (RH < 10 %) at 25 °C.".

3. L173: The term "κ-PDF" is introduced without definition. Please define it clearly upon first mention.

Response:

Thank you for this constructive suggestion. A clear definition of "κ-PDF" has been included at its first appearance in of the revised manuscript, as follows: "The κ probability density function (κ-PDF),

indicative of a statistical distribution that describes the variation in hygroscopicity among an aerosol population, was derived from the GF probability density function (GF-PDF), which was retrieved from the measured GF distribution function (GF-MDF) using the TDMAinv algorithm (Gysel et al., 2009).".

4. L197: Aerosols with diameters of 100 – 200 nm in number concentration typically represent secondary aerosols such as sulfate and nitrate, which often show mass size distribution peaks at 400 – 500 nm in previously published studies of AMS measurements. Could you provide the likely chemical composition of particles in the 100 – 200 nm range based on your measurements or referring to previous studies?

Response:

Thank you for this constructive suggestion. To elucidate the likely chemical composition of particles in the 100–200 nm range, we have incorporated a discussion referencing previous studies at Line 222 of the revised manuscript: "This finding on the other hand suggests that the larger particles (e.g., 100-200 nm) at the site, characterized by a higher degree of internal mixing, may stem from different origins and are most likely subject to long-range transport with extensive aging processes. This interpretation is supported in part by Li et al., (2011), who conducted measurements during similar seasons at Mt. Hua and reported that particles in the 100–400 nm range were predominantly composed of secondary inorganic species, such as SO_4^{2-}, NO_3^-, and NH_4^+, which typically have experienced longer aging processes."

5. Figure 2: Panels (a) to (e) show time series for particles from 30 nm to 200 nm, but the text within the panels is too small to read comfortably. Please enlarge the text for improved readability. Additionally, the term "URG" in the caption (and in line 235) might be better replaced with a descriptor indicating continuous or online measurement.

Response:

Thank you for this constructive suggestion. We have increased the font size of the text in all sub-panels of Figure 2 to enhance readability. In addition, we have replaced "URG" with "online measurement" in both the figure caption and in the revised manuscript to provide a clearer description of the data source.

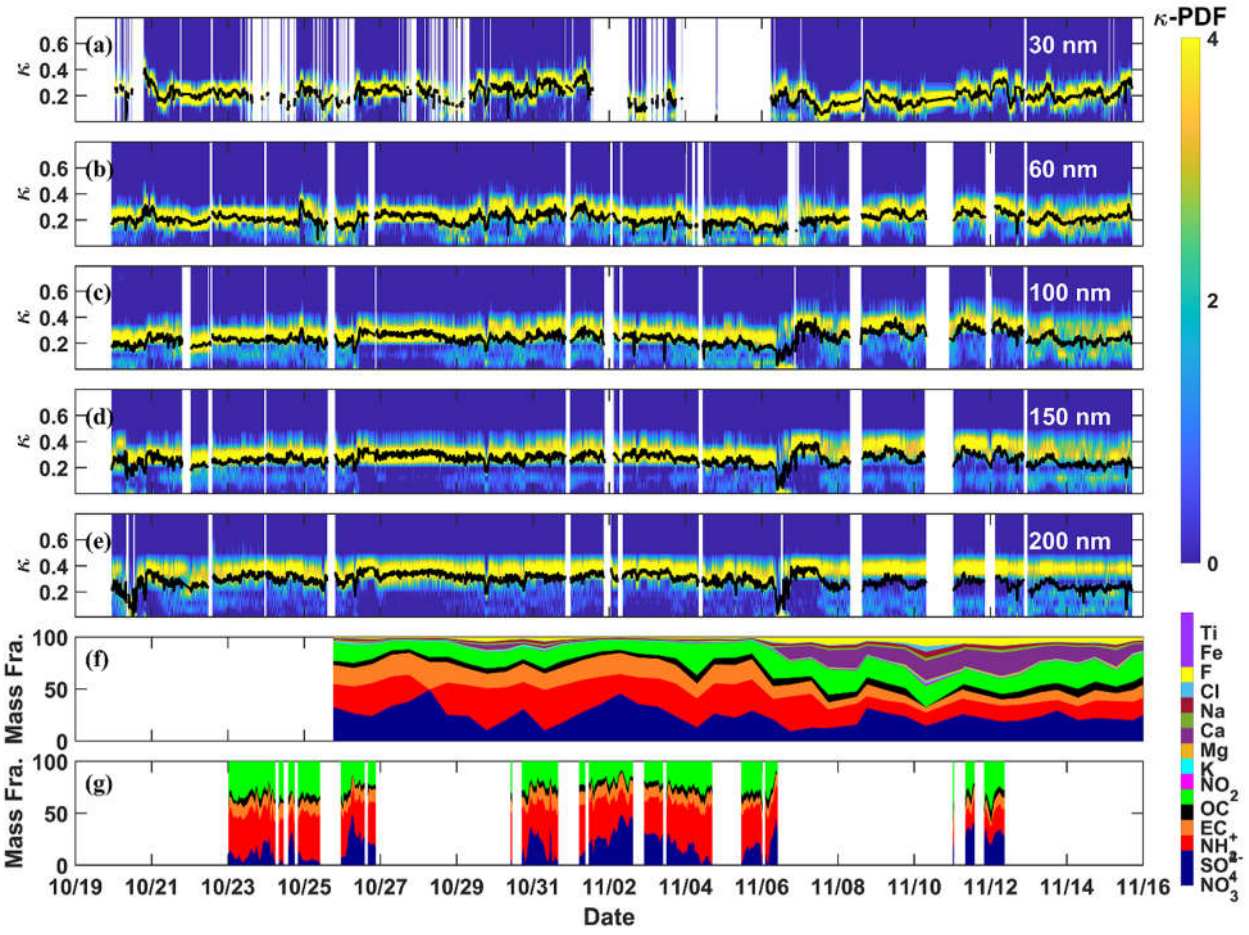

Figure 1. (a-e) Time series of κ-PDF for different particle sizes (with the black line indicating the mean κ value) and (f-g) Time series of chemical composition of $PM_{2.5}$ obtained using offline and continuous online measurements, respectively, during the sampling period.

6. Figure 2 (continued): Starting from November 14, a decrease in hygroscopicity (k) coincides with an increase in the mass fraction of elemental carbon (EC), particularly for particles in the 60 – 150 nm diameter range. Was this shift possibly associated with the advection of primary particles from urban areas? This period may serve as a useful contrast case relative to periods of higher hygroscopicity.

Response:

Thanks for this very constructive suggestion. In the original manuscript, we had discussed the influence of primary aerosols from domestic heating on the hygroscopicity during this period. However, we acknowledge that our description might have been too weak to clearly highlight this point. In response to your valuable comment, we have revised the entire paragraph as follows: "As noted earlier, beginning on November 6, which encompassed the entire duration of Cluster 3, 5, 1 DH, 2 DH, and 4 DH, regional domestic heating was initiated, which may emit substantial amounts of primary aerosols, such as black carbon (BC) and primary organic aerosols (POA). These aerosols were likely transported to our observational site via advection. This interpretation aligns with the findings of Du et al. (2022), who reported a marked increase in the fraction of organic aerosols as well as BC at Mt. Hua following the initiation of domestic heating. Though no direct source apportionment of organic aerosols can be

obtained by the current study, a moderate increase (approximately 7 %) in the organic mass fraction in $PM_{2.5}$ during Cluster 3 and 5, followed by a more pronounced rise in both organic (10 %) and BC fractions (5 %) during Cluster 1 DH, 2 DH, and 4 DH was observed compared to other clusters (see Fig.6), further supporting our previous hypothesis. Thus, the elevated levels of these primary aerosols, typically exhibited weak hygroscopicity (Shi et al., 2022), coupled with the high contents of weakly hygroscopic mineral dust, may synergistically drive the continued decline in aerosol hygroscopicity throughout this period."

7. Figures 4 and 6: Please consider enlarging the text in both figures to improve readability.

Response:

Thanks for your suggestion. We have enlarged the text in Figures 4 and 7 (formerly Figure 6) in the revised manuscript to improve readability. And the enlarged Figures are shown below.

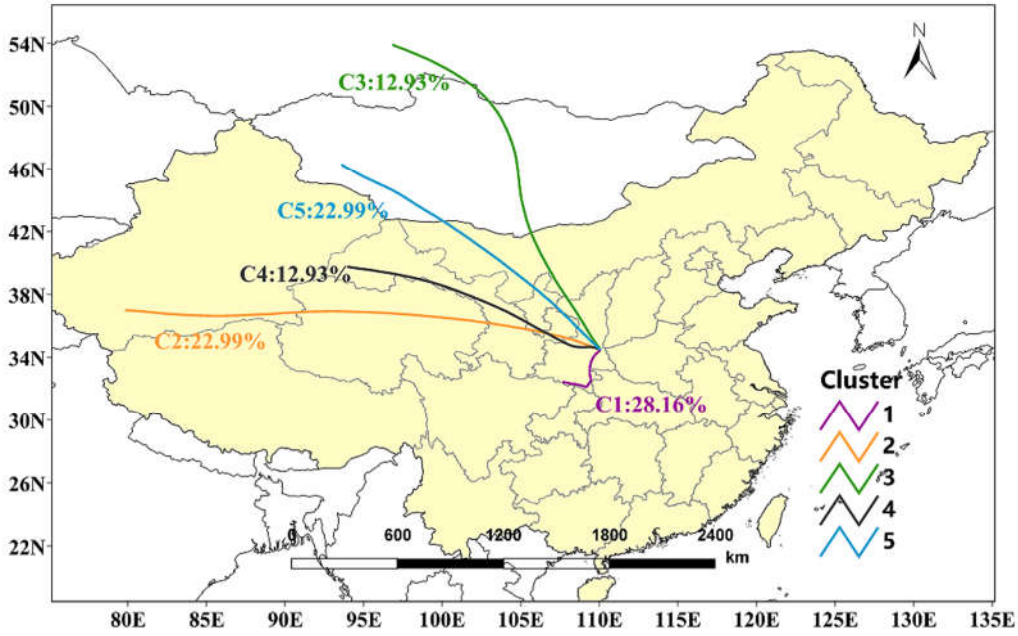

Figure 2. Cluster analysis of 72 h backward trajectories at 2060 m above ground level at the sampling site during the five trajectory-identified clusters. The line colors denote different clusters, i.e., purple for Cluster 1, yellow for Cluster 2, green for Cluster 3. black for Cluster 4, and blue for Cluster 5. (Figure 2 in manuscript)

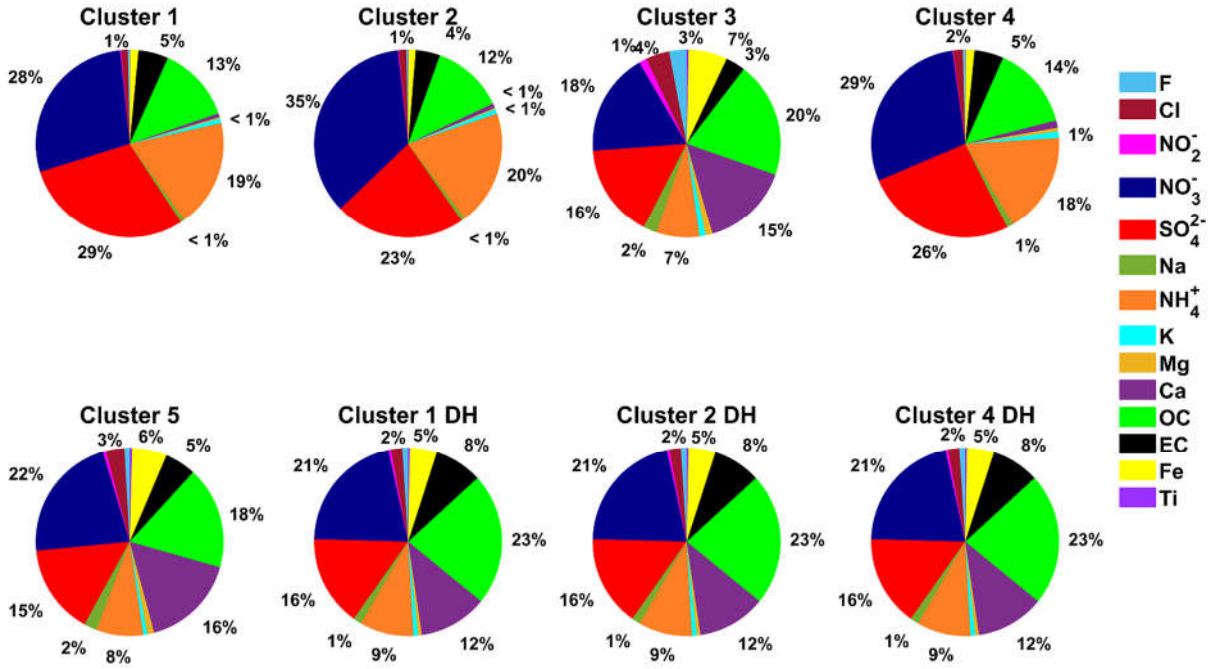

Figure 3. Proportions of chemical composition in different clusters. (Figure 6 in manuscript)

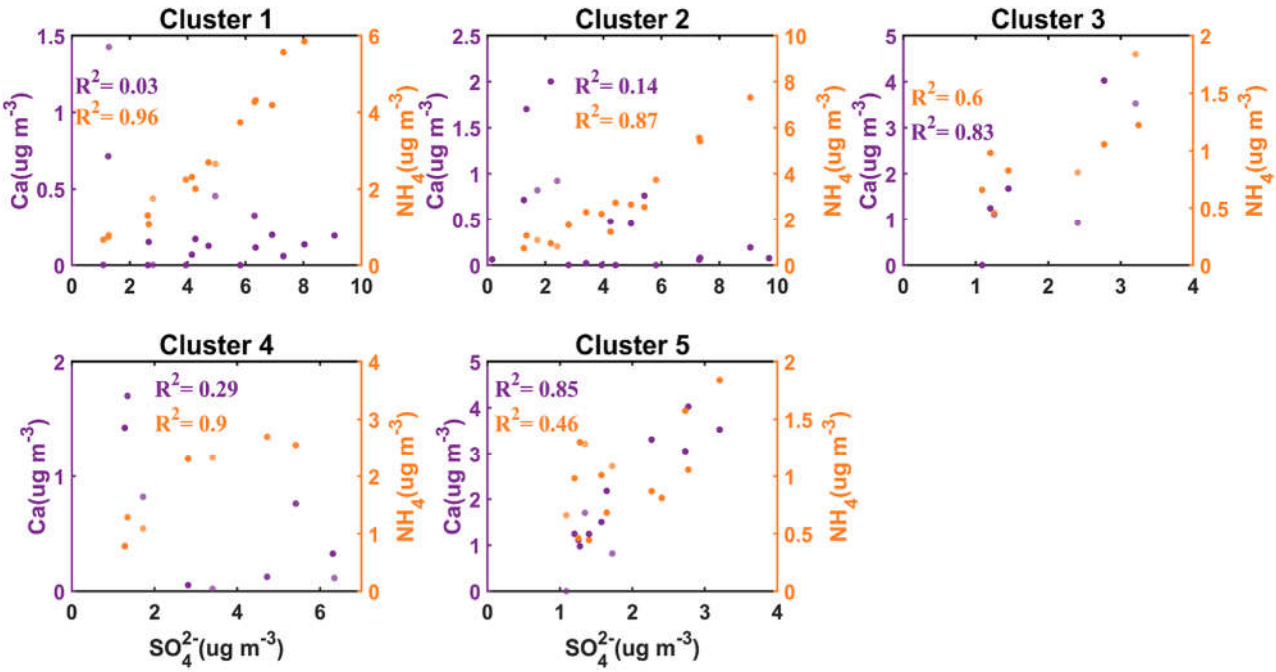

Figure 4. The correlation between $SO4^{2-}$ and Ca^{2+}, and $SO4^{2-}$ and NH_4^+ in $PM_{2.5}$ for different air masses. (Figure 7 in manuscript)

8. Figures 4 and 5: The six clusters identified in these figures appear to form two broad groups: clusters C3 and C5 versus the remaining clusters. Back-trajectory analysis in Figure 4 suggests that C3 and C5 are associated with air masses from cold and dry regions. In terms of k values, these clusters exhibit bimodal distributions, with lower values in the low hygroscopicity (LH) mode and higher values in the

moderate hygroscopicity (MH) mode for particles larger than 100 nm. Could the authors discuss how aerosol composition and hygroscopicity differ across these clusters?

Response: Thanks for the comments. We agree with the reviewer that the connection between aerosol composition and hygroscopicity is highly essential. Therefore, we have updated the trajectory analysis using 72-hour trajectories and made more discussions to relate aerosol composition with hygroscopicity across different clusters. The relevant part in Sect. 3.3 was revised as: "To comprehensively evaluate the impacts of long-range transport and regional emissions on aerosol hygroscopic properties, we compared the size-resolved aerosol hygroscopicity parameter (κ) across five air mass clusters identified through trajectory analysis (Fig.5a). As Cluster 1, 2 and 4 also occurred during the latter half of the campaign, coinciding with domestic heating activities, we further divided each of these three clusters into two distinct periods. The segments during the domestic heating period of these three clusters were specifically labeled as Cluster 1 DH, Cluster 2 DH and Cluster 4 DH, where "DH" denotes the influence of domestic heating. During the first half of the campaign, which was free from significant influence of mineral dust and prior to the onset of domestic heating activities (i.e., Cluster 1, 2, and 4), aerosols exhibited clear size-dependency of κ, with κ values increasing with increasing particle size. Moreover, the κ values observed for particles of the same sizes were relatively comparable across these three clusters. Air masses associated with these clusters, particularly Cluster 1, mainly transported over relatively short distances from southeastern and southwestern regions, passing through the heavily polluted Guanzhong Plain urban agglomeration and may represent the atmospheric conditions of this regional environment. In contrast, aerosols in Cluster 3, 5 and Cluster 1 DH, 2 DH, and 4 DH displayed relatively constant κ across most particle sizes, except for sub-100nm particles, which probably had local origins rather than long-range transport, as discussed earlier.

For 200 nm particles, Cluster 1, 2, and 4 exhibited the highest κ values (~0.32), followed by Cluster 3 and 5 (~0.27), while the lowest values were observed in Cluster 1 DH, 2 DH, and 4 DH (~0.22). Given that the chemical composition of bulk aerosols is more representative of larger particles than smaller ones (Hong et al., 2018), this pattern was consistent with the average aerosol composition measured by the online measurements. During Cluster 1, 2, and 4, aerosols were dominated by inorganic species, such as NH_4^+, SO_4^{2-}, NO_3^-, which are highly hygroscopic and accounted for over 70 % of the $PM_{2.5}$ mass fraction (see Fig.6).

For Cluster 3 and 5, the contribution of these inorganic species decreased markedly, dropping from over 70 % to less than 50 % in mass fraction, as shown in Fig.6. Concurrently, the levels of Ca^{2+}, Fe^{2+} increased substantially, from less 1 % to approximately 20 % of $PM_{2.5}$ mass. This shift may partially explain both the reduced hygroscopicity ($\kappa \approx 0.09$) and the elevated number fraction (21 %) of LH mode particles in these clusters compared to those ($\kappa \approx 0.12$, $NF_{LH} = 10$ %) in Cluster 1, 2, and 4, as these mineral dust components are generally hydrophobic or weakly hygroscopic. The influence of mineral dust was further confirmed by the strong correlation between SO_4^{2-} with Ca^{2+} ($R^2 = 0.83$) in Cluster 3 and 5, contrasting with their weak associations ($R^2 \approx 0.1$) during other clusters, where SO_4^{2-} was instead well linked to NH_4^+ ($R^2 \approx 0.9$) (see Fig.7). The co-variation of SO_4^{2-} and Ca^{2+} indicates that they possibly shared the same origins (Sullivan et al., 2009), with Ca^{2+} likely existing in the form of nearly non-hygroscopic $CaSO_4$ ($\kappa \approx 0.01$-0.05) during this episode, reinforcing the observed hygroscopicity decline relative to Cluster 1, 2, and 4. On the other hand, as particle size decreased, a slight increase in the overall aerosol hygroscopicity was observed in Cluster 3 and 5, which can be explained by the enhanced hygroscopicity of LH mode particles coupled with a small decrease in their number fraction. Given that mineral dust mainly resided in larger particles, this size-dependent trend in

hygroscopicity suggests a reduced contribution of mineral dust to the hygroscopicity of smaller particles within Cluster 3 and 5.

As noted earlier, beginning on November 6, which encompassed the entire duration of Cluster 3, 5, 1 DH, 2 DH, and 4 DH, regional domestic heating was initiated, which may emit substantial amounts of primary aerosols, such as black carbon (BC) and primary organic aerosols (POA). These aerosols were likely transported to our observational site via advection. This interpretation aligns with the findings of Du et al. (2022), who reported a marked increase in the fraction of organic aerosols as well as BC at Mt. Hua following the initiation of domestic heating. Though no direct source apportionment of organic aerosols can be obtained by the current study, a moderate increase (approximately 7 %) in the organic mass fraction in $PM_{2.5}$ during Cluster 3 and 5, followed by a more pronounced rise in both organic (10 %) and BC fractions (5 %) during Cluster 1 DH, 2 DH, and 4 DH was observed compared to other clusters (see Fig.6), further supporting our previous hypothesis. Thus, the elevated levels of these primary aerosols, typically exhibited weak hygroscopicity (Shi et al., 2022), coupled with the high contents of weakly hygroscopic mineral dust, may synergistically drive the continued decline in aerosol hygroscopicity throughout this period.

Despite both being influenced by dust events and domestic heating activities, aerosols in Cluster 5 exhibited higher aerosol hygroscopicity (0.25) compared to Cluster 3 (0.23), mainly due to their larger number fraction of MH mode particles, accompanied by the higher hygroscopicity of LH mode particles, as shown in Fig.5. Interestingly, striking high RH levels (around 80 %) were observed in Cluster 5, which nearly doubled the values in Cluster 3 (see Fig.S5). Such high-RH conditions may facilitate some specific aerosol processes, such as multi-phase or aqueous phase reactions, potentially altering their chemical composition and may explain their elevated hygroscopicity (Tong et al., 2020). This hypothesis aligns with the results of Du et al. (2022), who observed that the contribution of aqueous-formed water soluble oxidized organic aerosols to the total water-soluble organic aerosols increased from 11.21 % under low-RH levels to over 40 % at RH > 80 %, indicating a significant transformation in the organic aerosol composition. On the other hand, we noticed that the average κ of MH mode particles in Cluster 3 and 5 was markedly greater relative to other clusters (see Fig.5). Following our preceding reasoning, we suspected that the multi-phase or aqueous phase reactions under higher-RH levels in Cluster 5, not only enhanced the hygroscopicity of LH mode particles, but also produced substantial highly hygroscopic materials, which may have persisted until the entire duration of Cluster 3 and 5. However, without detailed compositional analysis at molecular level, the exact mechanisms responsible for this exceptionally high aerosol hygroscopicity remained unclear.

In summary, during the first half of the campaign, when air masses mainly passed through the heavily polluted Guanzhong Plain urban agglomeration, aerosols were primarily composed of secondary inorganic species and exhibited the highest hygroscopicity. Starting around November 6, increased influences from both mineral dust and domestic heating activities led to a noticeable decline in aerosol hygroscopicity, particularly in larger particles. This reduction was largely attributed to the rising levels of weakly hygroscopic components, such as mineral dust tracers (e.g., Ca^{2+}, Fe^{2+}), organic components as well as BC, highlighting the combined effects of long-range transport and regional emissions on aerosol composition and properties.".

9. I am not sure how this trajectory analysis can support aerosol hygroscopicity measurements, also as 6 clusters of air mass trajectories are not clearly distinguished and related to the aerosol measurements. Do the authors consider surface emissions based on trajectory height or microscale/synoptic meteorology

influencing aerosol hygroscopicity during transport? While I understand the manuscript is intended primarily as a measurement report, a brief discussion or summary connecting air mass origin, composition, and hygroscopic behavior would significantly enhance the interpretation of these results.

Response:

Thank you for your suggestion. We understand the reviewer's concern that the identified clusters of air mass trajectories may not be closely related to the aerosol measurements. As the reviewer previously noted, correlating aerosol hygroscopicity with their chemical composition would provide a more direct approach to evaluate the influence of different aerosol sources on their physicochemical properties. In response, we have revised Sect. 3.3 accordingly to improve the clarity and representation of these relationships. Additionally, we have included the vertical height profiles of the five air mass trajectories (see Fig.S6) and the time series of the boundary height at the site throughout the measurement period (see Fig.S7). The results indicate that all trajectories remained well above the boundary layer, suggesting that the observed air masses were not significantly influenced by local surface emissions. However, it is worth noting that these air masses passed through regions characterized by strong vertical mixing, such as those influenced by valley breeze, which could potentially uplift surface pollutants to the observational sites. At present, distinguishing such contributions remains challenging within our analysis.

As suggested by the reviewer, we have incorporated a brief summary at the end of Sect. 3.3 to better connect air mass origin, composition, and hygroscopic behavior to enhance the interpretation of the results. The summary is also provided below as: "In summary, during the first half of the campaign, when air masses mainly passed through the heavily polluted Guanzhong Plain urban agglomeration, aerosols were primarily composed of secondary inorganic species and exhibited the highest hygroscopicity. Starting around November 6, increased influences from both mineral dust and domestic heating activities led to a noticeable decline in aerosol hygroscopicity, particularly in larger particles. This reduction was largely attributed to the rising levels of weakly hygroscopic components, such as mineral dust tracers (e.g., Ca^{2+}, Fe^{2+}), organic components as well as BC, highlighting the combined effects of long-range transport and regional emissions on aerosol composition and properties.".

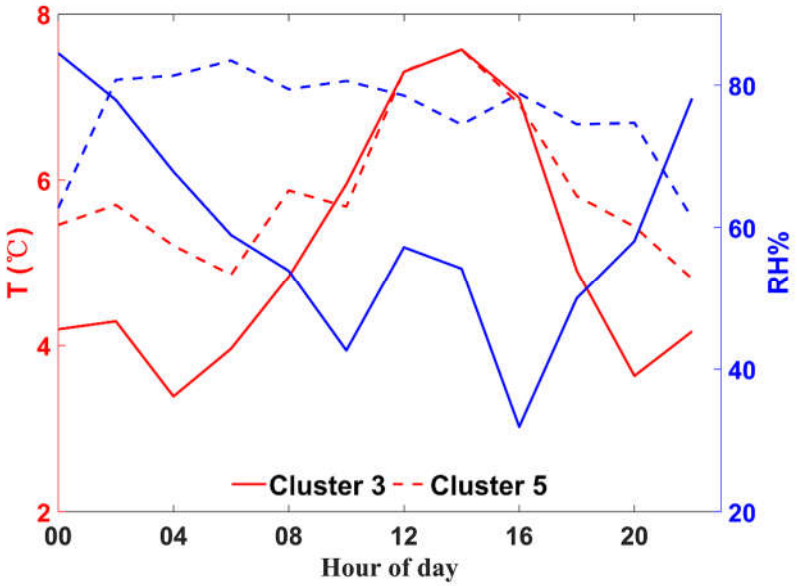

Figure 5. The diurnal variations in temperature and humidity for Cluster 3 and Cluster 5 during the

observation period.

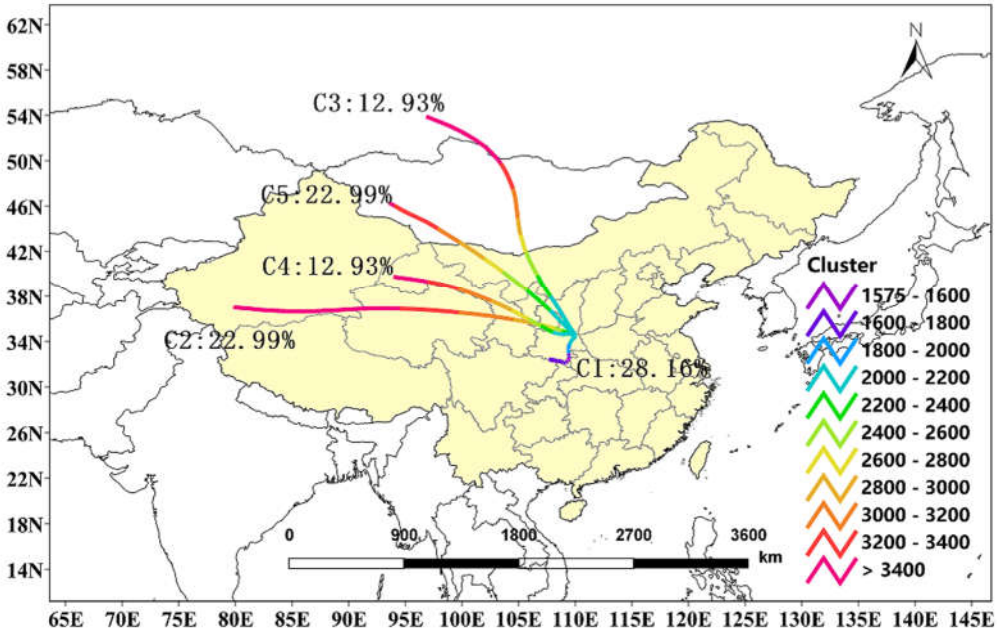

Figure 6. 72 h backward trajectory clusters at 2060 m above ground level. Different colors represent trajectory altitudes in distinct ranges. Percentages indicate the proportion of each cluster.

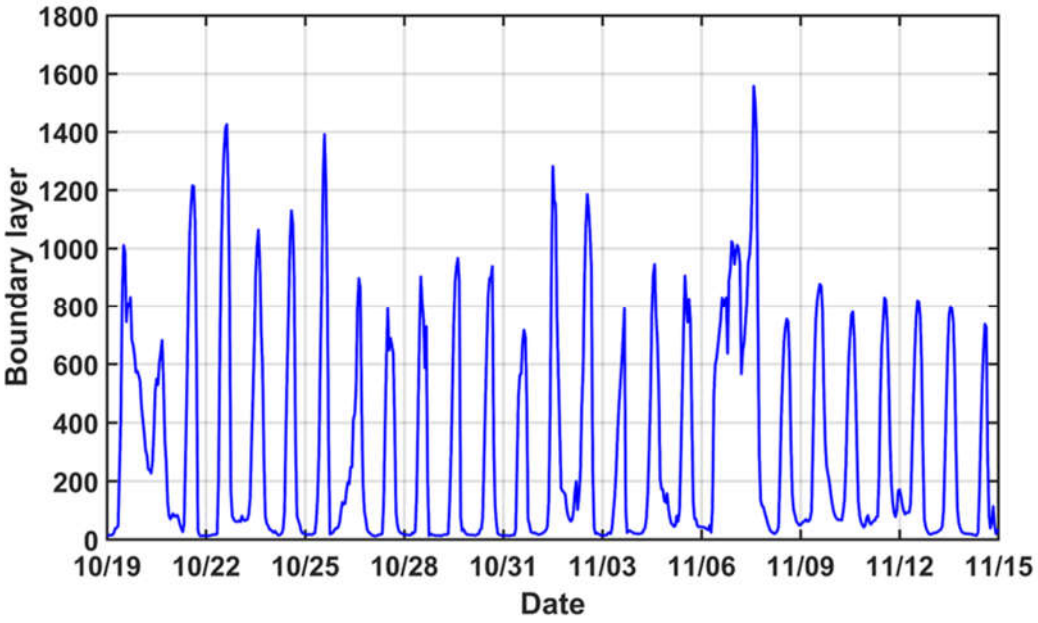

Figure 7. Time series of boundary layer height variations during the observation period.

References

Li, J., Wang, G., Zhou, B., Cheng, C., Cao, J., Shen, Z. and An, Z.: Chemical composition and size distribution of wintertime aerosols in the atmosphere of Mt. Hua in central China, Atmos. Environ., 45(6), 1251–1258, doi:10.1016/j.atmosenv.2010.12.009, 2011.

Du, A., Li, Y., Sun, J., Zhang, Z., You, B., Li, Z., Chen, C. and Li, J.: Rapid transition of aerosol optical properties and water-soluble organic aerosols in cold season in Fenwei Plain, Sci. Total Environ., 829, 154661, doi:10.1016/j.scitotenv.2022.154661, 2022.

Shi, J., Hong, J., Ma, N., Luo, Q., He, Y., Xu, H. and Tan, H.: Measurement report : On the difference in aerosol hygroscopicity between high and low relative humidity conditions in the North China Plain, Atmos. Chem. Phys., (22), 4599–4613, 2022.

Hong, J., Xu, H., Tan, H., Yin, C., Hao, L., Li, F., Cai, M., Deng, X., Wang, N., Su, H., Cheng, Y., Wang, L., Petäjä, T. and Kerminen, V. M.: Mixing state and particle hygroscopicity of organic-dominated aerosols over the Pearl River Delta region in China, Atmos. Chem. Phys., 18(19), 14079–14094, doi:10.5194/acp-18-14079-2018, 2018.

Sullivan, R. C., Moore, M. J. K., Petters, M. D., Kreidenweis, S. M., Roberts, G. C. and Prather, K. A.: Effect of chemical mixing state on the hygroscopicity and cloud nucleation properties of calcium mineral dust particles, Atmos. Chem. Phys., (9), 3303–3316, 2009.

Tong, Y., Pospisilova, V., Qi, L., Duan, J., Gu, Y., Kumar, V., Rai, P., Stefenelli, G., Wang, L., Wang, Y., Zhong, H., Baltensperger, U., Cao, J., Huang, R., Prevot, A. S. H. and Slowik, J. G.: Quantification of solid fuel combustion and aqueous chemistry contributions to secondary organic aerosol during wintertime haze events in Beijing, Atmos. Chem. Phys. Discuss., (August), 1–41, doi:10.5194/acp-2020-835, 2020.

Gysel, M., McFiggans, G. B. and Coe, H.: Inversion of tandem differential mobility analyser (TDMA) measurements, J. Aerosol Sci., 40(2), 134–151, doi:10.1016/j.jaerosci.2008.07.013, 2009.